Available online at www.sciencedirect.com
SCIENCE DIRECT
Journal of Asian Earth Sciences 27 (2006) 286–302
Journal of Asian Earth Sciences
www.elsevier.com/locate/jaes

Geochemical characteristics of the composite Kaçkar batholith generated in a Neo-Tethyan convergence system, Eastern Pontides, Turkey

Durmuş Boztuğ[a,*], A. İhsan Erçin[b], M. Kemal Kuruçelik[b], Deniz Göç[b], İsmail Kömür[b], Ali İskenderoğlu[b]

[a]*Department of Geological Engineering, Cumhuriyet University, 58140 Sivas, Turkey*
[b]*MTA Doğu Karadeniz Bölge Müdürlüğü, 61100 Trabzon, Turkey*

Received 21 November 2004; revised 3 December 2004; accepted 29 March 2005

Abstract

The composite Kaçkar batholith, of Cretaceous to Late Eocene age, consists of various intrusions derived from different geodynamic settings ranging from early to mature arc, through collision, to post-collisional extension in the Neo-Tethyan convergence system of the eastern Pontides of NE Turkey. The intrusions were emplaced into Cretaceous and Middle Eocene volcano-sedimentary units, and are unconformably overlain by Late Cretaceous, Early to Middle Eocene and Miocene units. The 10 lithological units are grouped into five geodynamic associations on the basis of geological setting and geochemical characteristics: (1) early arc origin as represented by the medium-K calc-alkaline (CALK) Çamlıkaya granitoid of Early Cretaceous age, (2) mature arc origin as represented by the medium- to high-K calc-alkaline Sırtyayla and Marselevat granitoids of Late Cretaceous to Early Palaeocene age, (3) syn-collisional plutonism as represented by the peraluminous Asniyor leucogranite of Palaeocene age, (4) post-collisional plutonism as represented by the high-K calc-alkaline Ayder K-feldspar megacrystic granitoid and the Sasmistal microgranite of Middle to Late Eocene age, (5) the extension-related, mildly alkaline Güllübağ monzonite, the medium-K calc-alkaline to slightly tholeiitic (THOL) Halkalıtaş quartz diorite, and the low-K tholeiitic Ardeşen gabbro and İsina diabase of Late Eocene age that are mainly exposed as small, shallow stocks and N–S, NE–SW, NW–SE and E–W trending veins.

Keywords: Geochemistry; Geodynamics; Granitoid; Kaçkar batholith; Eastern pontides; Turkey

1. Introduction

The Pontides of Turkey, particularly the eastern Pontides, represent a very well-preserved arc system (Eğin and Hirst, 1979; Manetti et al., 1983; Gedik et al., 1992; Çamur et al., 1994; Tokel, 1995; Yılmaz and Boztuğ, 1996; Boztuğ et al., 2001, 2002, 2003) resulting from northward subduction of the northern branch of Neo-Tethyan oceanic crust beneath the Eurasian plate (EP) along the Izmir-Ankara-Erzincan suture zone (IAESZ). The EP collided with the Tauride-Anatolide platform (TAP) in Late Palaeocene–Early Eocene time (Şengör and Yılmaz, 1981; Okay and Şahintürk, 1997; Yılmaz et al., 1997; Boztuğ et al., 2004).

The composite Kaçkar batholith has thus far been considered a single unit, Late Cretaceous to Early Tertiary in age (Gedik et al., 1992; Korkmaz et al., 1995; Okay and Şahintürk, 1997; Yılmaz et al., 1997, 2000). However, recent studies carried out by Yılmaz and Boztuğ (1996), Yılmaz et al. (2000), Boztuğ (2001), and Boztuğ et al. (2001, 2002, 2003) suggest the existence of collisional-related magmatism as well as arc-related igneous activity.

This paper deals mainly with the geological setting and main petrographical-chemical characteristics of the composite Kaçkar batholith, considered here to have been formed by different magmas derived from subduction, through collision, to extensional stages of the Neo-tethyan convergence system between Eurasia and the Tauride-Anatolide

* Corresponding author.
E-mail address: boztug@cumhuriyet.edu.tr (D. Boztuğ).

1367-9120/$ - see front matter © 2005 Elsevier Ltd. All rights reserved.
doi:10.1016/j.jseaes.2005.03.008

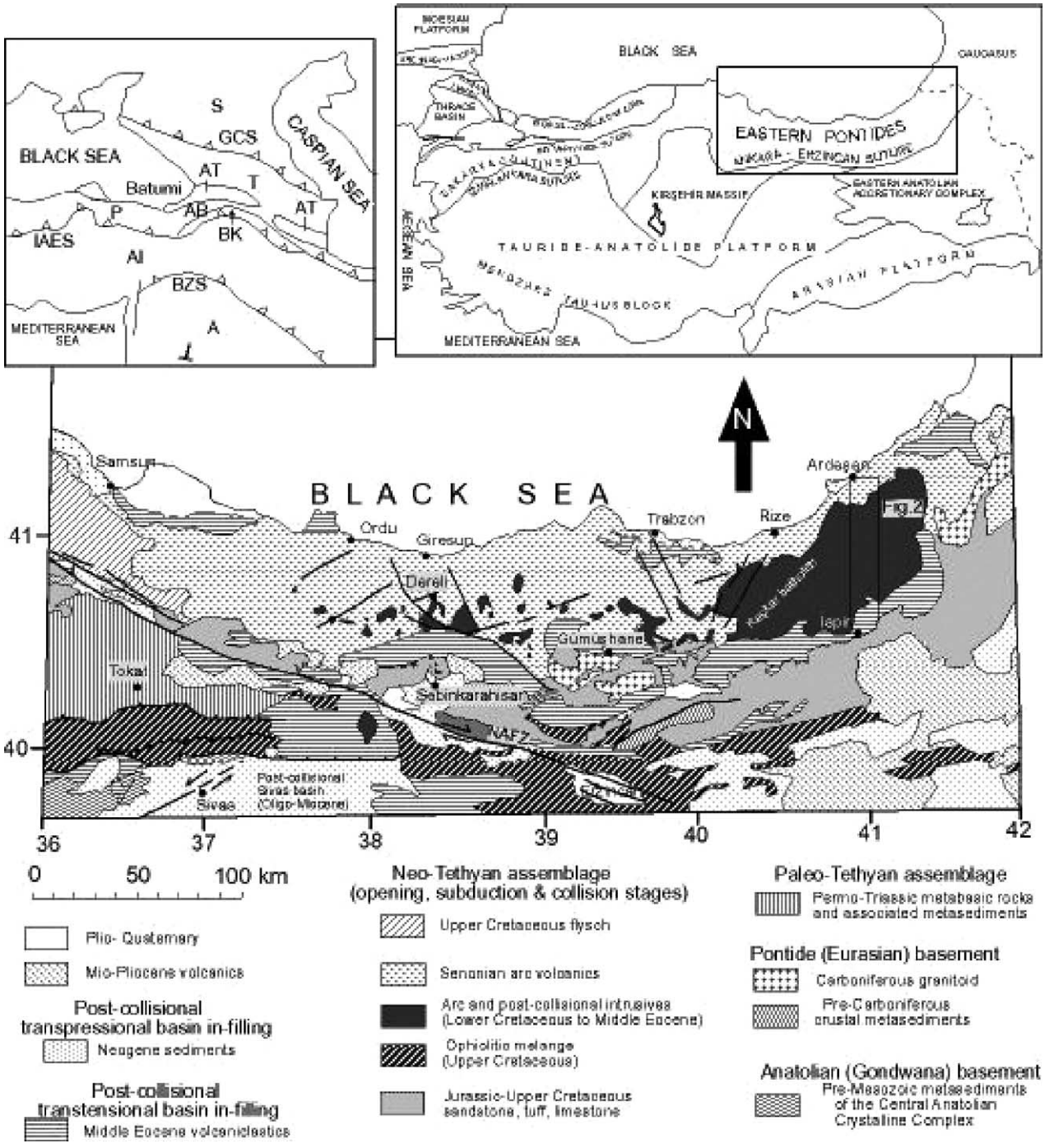

Fig. 1. Regional geological map of the eastern Black Sea region and location of the study area. The upper left and right insets showing the main tectonic units of Turkey and surrounding area are after Yılmaz et al. (2000); Yılmaz et al. (1997), respectively. Abbreviations in the upper left inset are as follows: S, Scythian platform; GCS, Greater Caucasus suture; AT, Adjara-Trialeti unit; T, Transcaucasus; P, Pontides; AB, Artvin-Bolnisi unit; BK, Bayburt-Karabagh imbricated unit; IAES, Izmir-Ankara-Erzincan suture; AI, Anatolian-Iran platform; BZS, Bitlis-Zagros suture; A, Arabian continent.

platform, from Early Cretaceous to Middle–Late Eocene time. A north to south geotraverse between the towns of Ardeşen (Rize) and İspir (Erzurum) in the eastern Black Sea region (Fig. 1) has been especially chosen for study in order to elucidate the broad spectrum of rocks that make up the Kaçkar batholith.

2. Analytical methods

Four hundred and one representative rock samples, collected from 10 different lithological units, have been analysed for whole-rock major-and trace-element geochemistry. The results are given in Table 1 as average values with

Table 1
Averages and standard deviations of the whole rock major (wt%) and trace element (ppm) chemical compositions of different intrusive rock units from the composite Kaçkar batholith

	Çamlıkaya					Sırtyayla				
	gd	to	qmzd	qd	mzgr	gd	mzgr	qmzd	qmz	gr
n	41	26	2	2	1	13	8	2	2	1
SiO_2	65.76	63.37	57.75	59.93	68.6	68.16	65.3	59.82	60.75	68.34
	(2.45)	(3.13)	(0.67)	(1.03)		(4.72)	(2.99)	(0.09)	(1.12)	
Al_2O_3	15.54	16.1	14.45	16.64	14.6	15.18	15.2	15.99	15.02	15.34
	(0.49)	(0.63)	(1.57)	(1.06)		(0.71)	(0.55)	(0.36)	(0.45)	
TiO_2	0.56	0.63	1.27	0.79	0.28	0.40	0.57	0.44	0.74	0.43
	(0.13)	(0.18)	(0.75)	(0.08)		(0.18)	(0.18)	(0.44)	(0.06)	
TFe_2O_3	3.95	4.5	7.64	5.81	2.3	3.79	4.58	5.79	3.47	3.57
	(0.79)	(1.38)	(2.21)	(0.11)		(1.65)	(1.12)	(0.11)	(0.79)	
MnO	0.07	0.08	0.15	0.11	0.05	0.09	0.1	0.12	0.12	0.08
	(0.02)	(0.03)	(0.02)	(0.01)		(0.04)	(0.02)	(0.01)	(0.01)	
MgO	2.58	3.21	4.66	3.35	1.	1.32	2.2	3.39	3.65	1.52
	(0.55)	(0.69)	(0.56)	(0.06)		(1.11)	(0.82)	(0.13)	(0.21)	
CaO	3.78	4.87	5.65	5.43	3.0	3.12	3.88	5.51	4.74	3.13
	(0.64)	(0.97)	(0.3)	(0.62)		(1.12)	(0.56)	(0.08)	(0.44)	
Na_2O	3.82	4.18	3.13	4.11	3.4	3.51	3.01	3.08	2.86	2.99
	(0.23)	(0.58)	(0.399)	(0.09)		(0.41)	(0.2)	(0.18)	(0)	
K_2O	2.71	1.54	2.49	1.94	4.48	3.41	3.94	3.46	4.25	4.34
	(0.34)	(0.53)	(0.13)	(0.42)		(0.33)	(0.14)	(0.03)	(0.6)	
P_2O_5	0.16	0.19	0.3	0.25	0.0	0.09	0.18	0.24	0.27	0.11
	(0.03)	(0.04)	(0.11)	(0.01)		(0.06)	(0.08)	(0.03)	(0.01)	
LOI	0.81	0.9	1.52	0.63	0.8	0.55	0.68	1.15	1.40	0.3
	(0.36)	(0.62)	(1.08)	(0.35)		(0.27)	(0.57)	(0.19)	(0.06)	
Total	99.74	99.59	98.98	98.96	99.39	99.62	99.63	98.97	99.25	100.15
	(0.58)	(0.54)	(0.27)	(0.47)		(0.45)	(0.44)	(0.54)	(0.2)	
Rb	58	19	23	37	173	123	125	108	119	157
	(19)	(17)	(20)	(18)		(28)	(24)	(11)	(18)	
Sr	398	500	461	479	273	249	381	620	552	293
	(51)	(82)	(131)	(66)		(65)	(101)	(42)	(2)	
Ba	564	370	375	431	987	899	754	698	614	830
	(121)	(127)	(146)	(102)		(165)	(238)	(7)	(16)	
Y	16	11	12	17	32	38	40	28	36	45
	(4)	(4)	(6)	(6)		(8)	(9)	(1)	(2)	
Zr	149	149	148	186	154	156	185	171	195	163
	(38)	(22)	(43)	(27)		(21)	(91)	(19)	(32)	
Nb	11	10	10	11	12	21	24	23	25	22
	(2)	(2)	(3)	(3)		(2)	(5)	(1)	(0)	
Th	10	5	5	8	18	17	23	18	26	18
	(6)	(3)	(8)	(1)		(8)	(12)	(2)	(2)	
Pb	9	6	6	4	37	29	29	32	30	28
	(9)	(2)	(2)	(0)		(2)	(3)	(1)	(1)	
Zn	51	59	57	65	78	77	80	87	84	75
	(9)	(14)	(18)	(4)		(6)	(5)	(1)	(6)	
Cr	29	34	34	32	32	8	9	6	41	nd
	(7)	(10)	(11)	(11)		(7)	(10)	(8)	(8)	
Co	47	37	35	35	30	129	95	72	66	126
	(17)	(12)	(12)	(1)		(46)	(33)	(1)	(11)	
Cu	16	15	16	26	13	35	49	62	66	31
	(10)	(8)	(10)	(18)		(89)	(14)	(4)	(21)	

	Marselevat							Asniyor			Ayder			
	gd	to	qmzd	qmz	mzgr	qd	d	mzgr	to	gr	mzgr	gd	gr	qmz
n	42	19	30	16	11	5	3	12	6	5	35	55	6	3
SiO_2	63.87	63.89	59.29	62.42	65.61	54.89	54.46	74.39	72.03	73.65	68.87	67.67	73.99	62.96
	(3.20)	(2.64)	(2.44)	(1.22)	(1.85)	(1.28)	(2.04)	(1.94)	(0.23)	(1.16)	(2.46)	(2.34)	(2.21)	(0.49)
Al_2O_3	15.62	15.69	16.26	15.83	15.47	16.72	17.58	14.29	14.41	14.22	14.82	15.12	14.04	16.06
	(0.60)	(0.64)	(0.57)	(0.30)	(0.20)	(0.66)	(1.21)	(0.80)	(0.68)	(1.02)	(0.40)	(0.46)	(0.56)	(0.63)
TiO_2	0.59	0.52	0.67	0.63	0.52	0.89	0.97	0.08	0.27	1.14	0.44	0.48	0.22	0.66

Table 1 (*continued*)

	Marselevat							Asniyor			Ayder			
	gd	to	qmzd	qmz	mzgr	qd	d	mzgr	to	gr	mzgr	gd	gr	qmz
	(0.14)	(0.10)	(0.09)	(0.07)	(0.06)	(0.18)	(0.52)	(0.07)	(0.12)	(0.06)	(0.12)	(0.11)	(0.10)	(0.08)
TFe_2O_3	4.81	5.22	6.26	4.48	3.38	7.81	7.58	0.89	0.95	1.05	2.79	3.13	1.28	4.33
	(1.34)	(1.52)	(0.41)	(0.68)	(0.81)	(0.43)	(0.15)	(0.34)	(0.37)	(0.40)	(0.87)	(0.94)	(0.73)	(0.39)
MnO	0.1	0.12	0.12	0.09	0.08	0.16	0.15	0.02	0.01	0.02	0.06	0.07	0.03	0.09
	(0.04)	(0.04)	(0.02)	(0.01)	(0.02)	(0.02)	(0.03)	(0.01)	(0)	(0.01)	(0.02)	(0.02)	(0.01)	(0.01)
MgO	2.75	2.54	3.37	3	2.18	4.32	4.82	0.88	2.01	0.93	1.44	1.68	0.36	2.7
	(0.70)	(0.67)	(0.59)	(0.30)	(0.53)	(0.72)	(0.61)	(0.19)	(0.70)	(0.18)	(0.60)	(0.56)	(0.42)	(0.52)
CaO	4.25	4.79	5.59	4.35	3.51	7.37	7.31	0.72	2.48	0.63	2.66	3.21	1.51	4.15
	(1.00)	(1.12)	(0.96)	(0.31)	(0.42)	(0.74)	(1.51)	(0.43)	(0.28)	(0.32)	(0.48)	(0.69)	(0.60)	(0.26)
Na_2O	3.5	3.83	3.19	3.22	3.14	3.55	4.21	4	5.85	3.2	3.5	3.75	3.11	3.33
	(0.45)	(0.64)	(0.51)	(0.16)	(0.26)	(0.43)	(0.51)	(0.24)	(0.44)	(0.56)	(0.26)	(0.32)	(0.39)	(0.04)
K_2O	2.93	1.36	3.27	4.4	4.57	1.38	1.33	4.33	0.47	5.23	4.28	3.56	5.07	4.65
	(0.71)	(0.66)	(0.45)	(0.24)	(0.39)	(0.35)	(0.82)	(0.39)	(0.11)	(0.39)	(0.27)	(0.40)	(0.18)	(0.15)
P_2O_5	0.17	0.14	0.24	0.24	0.18	0.28	0.32	0.03	0.07	0.04	0.17	0.19	0.05	0.23
	(0.04)	(0.03)	(0.05)	(0.02)	(0.04)	(0.07)	(0.15)	(0.02)	(0.03)	(0.02)	(0.04)	(0.04)	(0.06)	(0.02)
LOI	0.98	1.34	1.11	0.77	0.68	0.97	1.01	0.66	1.33	0.89	0.58	0.72	0.31	0.76
	(0.45)	(0.61)	(0.71)	(0.65)	(0.38)	(0.30)	(0.18)	(0.31)	(0.43)	(0.78)	(0.40)	(0.45)	(0.19)	(0.52)
Total	99.57	99.44	99.36	99.43	99.54	99.14	99.06	100.27	99.86	100	99.61	99.57	99.96	99.91
	(0.63)	(0.70)	(0.54)	(0.61)	(0.78)	(0.36)	(0.53)	(0.33)	(0.59)	(0.35)	(0.67)	(0.67)	(0.83)	(0.45)
Rb	75	43	80	132	144	25	26	177	16	116	165	141	216	141
	(25)	(18)	(21)	(29)	(21)	(20)	(23)	(54)	(18)	(39)	(28)	(35)	(46)	(36)
Sr	434	393	494	498	396	457	416	109	363	92	497	578	195	495
	(98)	(115)	(90)	(60)	(108)	(99)	(28)	(108)	(125)	(48)	(84)	(75)	(188)	(29)
Ba	645	516	760	634	662	378	250	453	95	954	547	537	447	609
	(182)	(252)	(193)	(74)	(194)	(194)	(84)	(406)	(33)	(580)	(131)	(102)	(207)	(106)
Y	24	21	26	31	40	15	16	37	10	19	43	36	48	37
	(9)	(10)	(5)	(6)	(6)	(3)	(10)	(13)	(10)	(9)	(6)	(8)	(7)	(10)
Zr	163	136	145	183	198	120	170	97	145	120	204	200	129	246
	(36)	(26)	(30)	(27)	(26)	(31)	(128)	(23)	(23)	(35)	(45)	(42)	(39)	(68)
Nb	17	16	16	18	21	10	11	27	15	18	33	30	31	24
	(5)	(5)	(5)	(7)	(6)	(5)	(10)	(21)	(1)	(10)	(3)	(6)	(7)	(12)
Th	11	5	10	20	25	3	3	27	19	23	45	38	47	24
	(7)	(4)	(5)	(6)	(4)	(2)	(2)	(11)	(5)	(8)	(11)	(13)	(12)	(9)
Pb	17	19	27	35	28	11	7	22	8	9	29	28	30	23
	(11)	(9)	(9)	(13)	(5)	(11)	(6)	(16)	(3)	(4)	(2)	(4)	(1)	(2)
Zn	68	72	82	79	69	78	79	39	32	36	72	75	66	85
	(17)	(16)	(11)	(12)	(10)	(10)	(27)	(11)	(2)	(5)	(4)	(5)	(6)	(4)
Cr	20	15	28	35	22	30	24	29	33	27	10	10	10	28
	(14)	(12)	(33)	(10)	(16)	(26)	(12)	(8)	(5)	(5)	(7)	(10)	(7)	(18)
Co	60	68	51	55	74	30	29	69	57	48	118	111	165	62
	(29)	(26)	(18)	(18)	(32)	(11)	(11)	(27)	(13)	(5)	(22)	(36)	(30)	(28)
Cu	44	31	67	53	45	49	57	18	13	16	39	41	28	58
	(40)	(12)	(53)	(13)	(20)	(27)	(43)	(8)	(1)	(6)	(25)	(27)	(3)	(27)

	Sasmistal			Halkalıtas			Güllübağ			Ardesen	Isina
	gr	mzgr	gd	qd	d	to	mz	qmz	qmzd	go	qd
n	14	2	1	13	5	3	5	5	2	2	3
SiO_2	75.54	75.27	68.99	52.34	47.69	60.28	59.03	60.51	58.92	45.78	48.87
	(1.21)	(0.06)		(2.67)	(3.99)	(3.20)	(1.83)	(1.33)	(2.34)	(0.33)	(2.26)
Al_2O_3	13.9	14.32	14.89	17.43	17.72	16.33	17.26	16.65	16.66	11.85	16.6
	(0.49)	(0.11)		(0.60)	(1.91)	(0.68)	(0.39)	(0.14)	(0.97)	(2.59)	(3.02)
TiO_2	0.12	0.17	0.43	0.88	0.71	0.56	0.76	0.64	0.68	0.72	0.81
	(0.04)	(0.03)		(0.25)	(0.23)	(0.13)	(0.07)	(0.05)	(0.13)	(0.07)	(0.32)
TFe_2O_3	0.44	1.04	2.71	9.02	9.63	6.9	5.22	4.68	5.41	11.36	10.8
	(0.40)	(0.06)		(1.38)	(1.80)	(1.00)	(0.45)	(0.50)	(1.29)	(0.35)	(2.92)
MnO	0.02	0.02	0.09	0.18	0.19	0.14	0.09	0.09	0.12	0.2	0.18
	(0.01)	(0.01)		(0.03)	(0.01)	(0.07)	(0.01)	(0.01)	(0.01)	(0.02)	(0.06)
MgO	0.12	0.34	1.86	5	8.1	3.2	3.23	3.15	3.38	12.71	5.73
	(0.30)	(0.37)		(0.95)	(3.75)	(0.24)	(0.66)	(0.48)	(1.46)	(0.53)	(2.57)

(*continued on next page*)

Table 1 (*continued*)

	Sasmistal			Halkalıtas			Güllübağ			Ardesen	Isina
	gr	mzgr	gd	qd	d	to	mz	qmz	qmzd	go	qd
CaO	0.79	1.01	2.82	9.17	11.2	5.49	4.87	4	5.7	13.68	9.17
	(0.13)	(0.29)		(0.43)	(2.34)	(2.12)	(0.63)	(0.54)	(0.66)	(1.74)	(2.88)
Na_2O	3.27	3.57	4.13	2.89	2.4	3.79	4.25	3.89	3.8	1.01	2.64
	(0.26)	(0.12)		(0.54)	(1.51)	(1.15)	(0.19)	(0.18)	(0.01)	(0.48)	(0.90)
K_2O	5.34	4.22	3	0.8	0.42	1.06	4.19	4.4	3.5	0.19	0.11
	(0.23)	(0.31)		(0.61)	(0.64)	(0.54)	(0.36)	(0.36)	(0.82)	(0.25)	(0.18)
P_2O_5	0.03	0.05	0.19	0.26	0.12	0.14	0.43	0.29	0.32	0.1	0.15
	(0.01)	(0.02)		(0.12)	(0.10)	(0.01)	(0.08)	(0.04)	(0.04)	(0.04)	(0.06)
LOI	0.38	0.34	0.69	1.19	1.06	0.89	0.37	0.85	1.61	1.58	4.13
	(0.38)	(0.28)		(0.91)	(0.30)	(0.22)	(0.34)	(0.51)	(0.43)	(0.35)	(0.44)
Total	99.94	100.33	99.3	99.15	99.24	99.28	99.7	99.14	100.07	99.17	99.18
	(0.62)	(0.13)		(0.35)	(0.23)	(0.38)	(0.85)	(0.23)	(0.98)	(0.02)	(0.15)
Rb	211	172	115	40	24	51	127	161	95	30	32
	(62)	(75)		(13)	(14)	(16)	(29)	(32)	(56)	(1)	(5)
Sr	47	206	568	449	486	382	445	476	471	169	154
	(67)	(12)		(11)	(64)	(15)	(13)	(38)	(4)	(65)	(113)
Ba	324	457	449	449	241	431	535	591	518	174	184
	(212)	(144)		(217)	(50)	(287)	(60)	(32)	(46)	(28)	(30)
Y	47	34	49	18	10	22	32	36	27	6	12
	(15)	(20)		(5)	(3)	(9)	(4)	(5)	(11)	(1)	(5)
Zr	98	132	181	89	53	125	245	261	210	23	40
	(26)	(13)		(47)	(17)	(24)	(35)	(43)	(44)	(8)	(14)
Nb	30	25	35	17	12	15	14	17	14	17	16
	(10)	(13)		(1)	(7)	(5)	(3)	(3)	(4)	(1)	(1)
Th	45	40	47	2	1	8	12	16	14	3	2
	(15)	(13)		(2)	(1)	(4)	(4)	(5)	(13)	(4)	(3)
Pb	30	24	27	23	18	18	28	36	35	22	22
	(7)	(5)		(7)	(8)	(10)	(4)	(10)	(1)	(0)	(1)
Zn	57	52	79	86	77	71	65	70	73	82	80
	(10)	(15)		(9)	(7)	(26)	(6)	(2)	(8)	(5)	(13)
Cr	7	24	11	14	92	8	20	19	23	303	53
	(9)	(19)		(41)	(157)	(14)	(3)	(2)	(11)	(40)	(91)
Co	163	119	133	43	39	63	21	23	24	58	43
	(64)	(63)		(11)	(16)	(30)	(4)	(5)	(2)	(4)	(10)
Cu	33	25	29	47	75	34	110	78	79	49	37
	(10)	(11)		(18)	(52)	(19)	(36)	(24)	(12)	(5)	(11)

Explanations: n, sample number; the numbers given in parentheses below each value correspond to the standard deviation; tFe_2O_3, total iron oxide as ferric iron; LOI, loss on ignition; gd, granodiorite; to, tonalite; qmzd, quartz monzodiorite; qd, quartz diorite; mzgr, monzogranite; gr, granite; d/go, diorite/gabbro; nd, not determined.

standard deviations for each rock type from all lithological units. The geochemical analyses were carried out on pressed powder tablets using X-ray fluorescence spectrometry (Rigaku 3270 E-WDS) at the Mineralogical–Petrographical and Geochemical Research Laboratories (MIPJAL) of the Department of Geological Engineering, Cumhuriyet University (Sivas) using USGS and CRPG rock standards for calibration. Analytical results from USGS, CRPG and GIT-IWG standards obtained by MIPJAL and their recommended values by Govindaraju (1989) are also given in Table 2.

3. Geological setting

An area of approximately 1800 km^2 was first mapped geologically at a scale of 1:25,000 (Fig. 2), and 10 lithological units belonging to five different magmatic episodes of the Kaçkar batholith were identified. The oldest intrusive unit is the Çamlıkaya granitoid of Early Cretaceous age (Boztuğ et al., 2002). It is unconformably overlain by the Upper Cretaceous (Turonian) Ardıçlı Formation, comprising mainly red, coarse-grained sandstone, sandstone, siltstone, marl and scarce coal units. Widespread arc-volcanic rocks are represented, from bottom to top, by the Çatak, Kızılkaya and Çağlayan volcano-sedimentary formations of Maastrichtian age. These units consist essentially of submarine volcanic eruptions associated with epiclastic and calcareous sediments. They unconformably overlie the Çamlıkaya granodiorite and Ardıçlı Formation (Fig. 2). The second intrusive episode is represented by the Sırtyayla and Marselevat granitoids of Late Cretaceous to Early Palaeocene age (Boztuğ et al., 2002). These rocks intrude the Çamlıkaya granitoid and Çağlayan Formation. Intrusion of the Marselevat granitoid into the Sırtyayla granitoid is exposed in the road cut between the town of Çamlıhemşin

Table 2
Comparision of the geochemical analyses results of the GIT-IWG, CRPG and USGS rock standards by Sivas-MIPJAL and their recommended values by Govindaraju (1989). Major and trace elements are given in wt (%) and ppm, respectively

Standards	GIT-IWG	MİPJAL	CRPG	MİPJAL	CRPG	MİPJAL	CRPG	MİPJAL	USGS	MİPJAL	USGS	MİPJAL
	AC-E	AC-E	GA	GA	GH	GH	BR	BR	SCo-1	SCo-1	AGV-1	AGV-1
SiO_2	70.35	68.18	69.90	69.71	75.80	76.08	38.20	38.33	62.78	63.72	58.79	58.59
TiO_2	0.11	0.09	0.38	0.36	0.08	0.06	2.60	2.49	0.63	0.68	1.05	1.08
Al_2O_3	14.70	14.42	14.50	15.33	12.50	11.33	10.20	9.90	13.67	14.43	17.14	16.12
tFe_2O_3	2.53	2.83	2.83	2.45	1.34	1.32	12.88	10.13	5.14	5.78	6.76	6.45
MnO	0.06	0.06	0.09	0.09	0.05	0.05	0.20	0.17	0.05	0.06	0.09	0.10
MgO	0.03	0.51	0.95	1.41	0.03	0.60	13.28	13.20	2.72	3.20	1.53	1.42
CaO	0.34	0.44	2.45	2.36	0.69	0.82	13.80	14.23	2.62	3.26	4.94	4.75
Na_2O	6.54	6.56	3.55	3.53	3.85	3.17	3.05	3.19	0.90	0.63	4.26	3.78
K_2O	4.49	4.42	4.03	4.23	4.76	4.45	1.40	1.62	2.77	2.98	2.91	2.89
P_2O_5	0.01	0.02	0.12	0.15	0.01	0.02	1.04	1.44	0.21	0.20	0.49	0.48
LOI	0.37	0.51	1.00	0.87	0.70	0.81	3.00	3.17	6.66	6.10	1.20	1.42
Total	99.53	98.04	99.80	100.49	99.81	98.71	99.65	97.87	98.15	101.04	99.16	97.08
Cu	4	13	16	13	14	13	72	38	29	28	60	46
Pb	39	39	30	26	45	39	8	5	31	41	36	28
Zn	224	216	80	73	85	77	160	94	103	105	88	82
Rb	152	148	175	177	390	294	47	13	127	105	67	47
Ba	55	80	840	852	20	19	1050	786	570	584	1226	1161
Sr	3	5	310	317	10	11	1320	827	174	169	662	555
Nb	110	98	12	11	85	80	98	52	11	12	15	10
Zr	780	780	150	150	150	146	250	205	160	160	227	212
Y	184	181	21	22	75	129	30	23	26	29	20	15
Th	18.5	18	17	15	87	70	11	9	9	7	6	4

and Ayder Yayla, and is the youngest of the rocks of this episode. Both the Marselevat and Sırtyayla granitoids contain ovoidal- to ellipsoidal-shaped, mafic, microgranular enclaves (MME) (Didier and Barbarin, 1991; Barbarin and Didier, 1992) with dimensions ranging from a few cm to 1–2 dm in the field. A huge leucocratic granite outcrop, constituting the third intrusive pulse, and called the Asniyor leucogranite, intrudes both the Çamlıkaya and Marselevat granitoids (Fig. 2).

The fourth intrusive pulse is represented by the Ayder K-feldspar megacrystic granitoid and the Sasmistal microgranite of Middle to Late Eocene age (Boztuğ et al., 2002). The Ayder granitoid intrudes the Çağlayan Formation and the Marselevat and Sırtyayla granitoids (Fig. 2). The most diagnostic field characteristics of this unit are the large, pinkish K-feldspar megacrysts and widespread MMEs, including composite MME occurrences with various ovoidal, ellipsoidal and even angular shapes, and having diameters up to several dm. These MMEs represent mingling between coeval mafic and felsic magmas (Didier and Barbarin, 1991; Barbarin and Didier, 1992). The Sasmistal microgranite is generally exposed as N–S trending, small subvolcanic emplacements mainly within the Ayder granitoid, and locally within the Asniyor leucogranite (Fig. 2). A volcano-sedimentary sequence—which contains Middle Eocene fossils—with a basal conglomerate unit, called the Kabaköy Formation, unconformably overlies the Çamlıkaya granitoid (Fig. 2).

The Güllübağ monzonite and the Halkalıtaş quartz diorite of Late Eocene age (Boztuğ et al., 2002) are exposed as small stocks and some subvolcanic dikes with N–S, NE–SW, NW–SE and E–W orientations (Fig. 2). These are considered to represent an extension-related fifth intrusive pulse. Other mafic and basic small gabbroic stocks and dike rocks with the same orientations, namely the Ardeşen gabbro and İsina diabase, are also considered to be part of the fifth igneous pulse (Fig. 2). All of these intrusive rocks and wall rocks are unconformably overlain by Miocene molasse-type sediments consisting of alternating conglomerate, sandstone, siltstone, claystone and marl (Fig. 2). The Guvant andesitic tuff is exposed along a major fault plane (Fig. 2) and is similar to tuffs of the İkizdere-Rize area in the eastern Pontides; thus, the Guvant andesitic tuff is correlated with the İkizdere-Rize volcanic rocks. The latter is a neotectonic eruption, with fission-track ages of some fracture-filling obsidians indicating a Plio-Pleistocene age (Yeğingil et al., 2002).

The major structural elements of the study area consist of NE–SW-trending faults and NW-SE-trending fold axes. The former tectonically exhumed the Kaçkar batholith sometime around Miocene time as indicated by apatite fission-track data (work in progress). Miocene denudation has also been documented by Yılmaz et al. (1997) in the Pontide mountain belt as erosion of a giant horst block. There are also some significant secondary faults that trend mainly E–W.

4. Petrography

Rock nomenclature has been determined through a combination of petrography and major-element

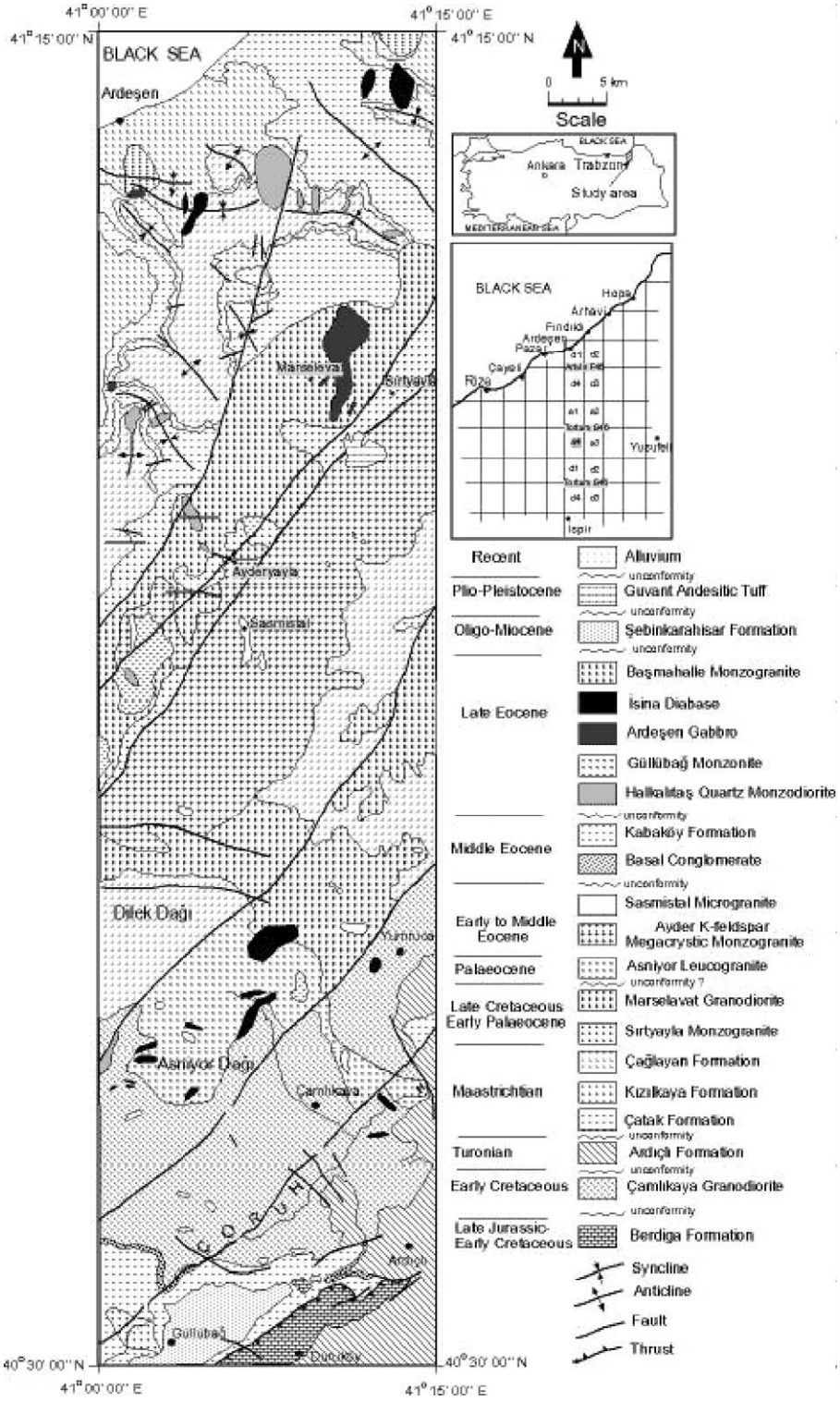

Fig. 2. Geological map of the composite Kaçkar batholith along a N–S geotraverse between Ardeşen (Rize) and İspir (Erzurum) towns, eastern Black Sea region, Turkey.

geochemical data following the classification suggested by Debon and Le Fort (1983). The four intrusive associations, as determined by microscopic and whole-rock geochemical studies of the Kaçkar batholith, are as follows: (1) an arc-related intrusive association, (2) the syn-collisional Asniyor leucogranite, (3) a post-collisional high-K calc-alkaline intrusive association, and (4) an extension-related intrusive association. The main petrographic characteristics of these intrusive associations are summarized below.

4.1. Subduction related intrusive association

This intrusive association comprises the Çamlıkaya granitoid (Early Cretaceous) and Sırtyayla and Marselevat granitoids (Late Cretaceous–Early Palaeocene). The Çamlıkaya and Marselevat granitoids typically have medium-grained equigranular textures characterized by quartz, plagioclase, orthoclase, hornblende, biotite and clinopyroxene as major constituents, along with accessory phases such as apatite, titanite, zircon, epidote and opaque minerals. The Sırtyayla granitoid differs from them in terms of both texture and mineralogical composition. The Sırtyayla granitoid has coarse-grained texture characterized by large feldspar crystals, and typically contains more biotite than hornblende in its modal composition. The Çamlıkaya, Sırtyayla and Marselevat granodiorites contain different types of MMEs in the field, and some special microscopic textures, such as anti-rapakivi texture, bladed biotite, poikilitic/oikocrystic quartz and K-feldspars, biotite/hornblende zone in K-feldspar phenocrysts, small lath-shaped plagioclase and boxy cellular growth plagioclase occurrences as described by Hibbard (1991, 1995), which reflect mingling and mixing between coeval felsic and mafic magmas (Didier and Barbarin, 1991; Barbarin and Didier, 1992). The chemical nomenclature diagram (Table 1, Fig. 3) mainly shows granodioritic compositions for the Çamlıkaya, Sırtyayla and Marselevat granitoids. However other rock types are also present. Tonalite samples from the Çamlıkaya and Marselevat granitoids are not true tonalites [even though they plot in the tonalite field of the chemical nomenclature diagram of Debon and Le Fort (1983)] due to high Na content (and Ca only in the Çamlıkaya unit) along with lesser amounts of K. Such K depletion is consistent with decrease in Rb in the tonalite samples, more or less reduced by half relative to the granodiorite (Table 1).

4.2. Syn-collisional asniyor leucogranite

The Asniyor leucogranite has equigranular to porphyritic textures consisting of quartz, orthoclase, plagioclase and chloritized biotite (which are scarce in the modal mineralogical composition). There is widespread hydrothermal alteration in the Asniyor leucogranite which resulted in alteration of feldspars to kaolinite and sericite. Most of the samples plot in the adamellite and granite fields in the chemical nomenclature diagram (Fig. 3). Debon and Le Fort (1983) point out that their adamellite includes monzogranites of Streckeisen (1976). They used the term of adamellite instead of monzogranite or monzonitic granite in order to avoid confusion with the quartz monzonite and monzonitic associations (Debon and Le Fort, 1983, p. 136). Thus, the rock samples plotted in the adamellite subfield in Fig. 3 are termed monzogranite in this study. Some samples of Asniyor leucogranite plot in the tonalite field, similar to tonalites of the arc-related intrusive association due to their high Na contents and depletion in K (Table 1 and Fig. 3). The depletion in K parallels Rb depletion and may indicate late-stage hydrothermal activity which resulted in removal of K and Rb and enrichment in Na.

4.3. Post-collisional high-K calc-alkaline intrusive association

The Ayder K-feldspar megacrystic granitoid typically has porphyritic texture characterized by the presence of

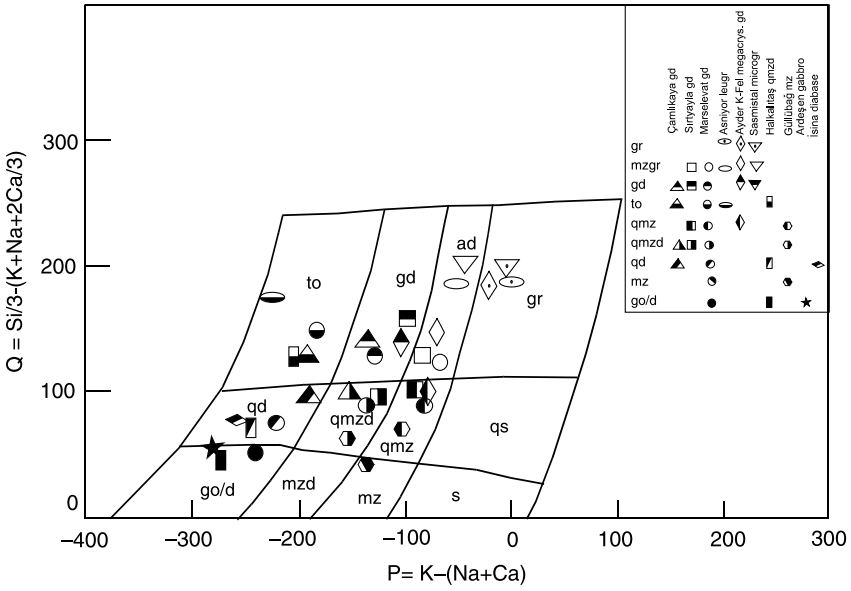

Fig. 3. Chemical nomenclature diagram (Debon and Le Fort, 1983) for rock samples from the Kaçkar batholith. gr, granite; ad, adamellite (monzogranite); gd, granodiorite; to, tonalite; qs, quartz syenite; qmz, quartz monzonite; qmzd, quartz monzodiorite; qd, quartz diorite; s, syenite; mz, monzonite; mzd, monzodiorite; go/d, gabbro/diorite.

K-feldspar megacrysts up to 4–5 cm in length and 1–2 cm in width. These K-feldspar megacrysts also include widespread ferromagnesian minerals such as amphibole, pyroxene and biotite, some of which are visible in hand specimen. The major rock-forming minerals of this unit include quartz, orthoclase, plagioclase, hornblende, biotite and augite. The accessory phases consist of apatite, allanite, titanite, zircon and opaque minerals. The MMEs, locally containing K-feldspar megacrysts resembling those of the host rock, are typical in the Ayder K-feldspar megacrystic granitoid. These megacrysts are indicative of thermal, mechanical and chemical interaction between coeval mafic and felsic magma sources (Barbarin and Didier, 1992). Apart from these occurrences, some special microscopic textures, such as spongy cellular dissolution/melting plagioclase, boxy cellular growth plagioclase, anti-rapakivi texture and poikilitic/oikocrystic K-feldspars, as described by Hibbard (1991, 1995), suggest magma mixing in the Ayder K-feldspar megacrystic granitoid. The Sasmistal microgranite, cropping out as N–S- trending subvolcanic intrusions within the Ayder K-feldspar megacrystic granitoid, consists mainly of quartz, orthoclase, plagioclase and lesser amounts of biotite with a phaneritic or locally aphanitic and porphyritic texture.

4.4. Extensional related intrusive association

This association consists of four mappable lithological units: the Güllübağ monzonite, the Halkalıtaş quartz diorite, the Ardeşen gabbro and the Isina diabase, all of which are exposed as shallow-seated small stocks and dikes with typical porphyritic texture except for the Ardeşen gabbro. This porphyritic texture is characterized by lath-shaped plagioclase in a groundmass of plagioclase, orthoclase, amphibole, augite and biotite in the Güllübağ monzonite, and by the presence of large plagioclase, hornblende and augite phenocrysts in a phaneritic groundmass consisting of feldspar and mafic minerals in the Halkalıtaş quartz diorite and Isina diabase. The Ardeşen gabbro is equigranular and coarse- grained and locally is characterized by an intercumulus texture consisting of augite, plagioclase and some relict olivine, with accessory apatite and opaque minerals.

5. Main geochemical characteristics

The main geochemical characteristics of the intrusive associations of the composite Kaçkar batholith, from oldest to youngest, are summarized below.

5.1. Subduction related intrusive association

Major-element geochemical data indicate a subalkaline-calc-alkaline composition for the arc-related intrusive association (Fig. 4). The diorites and quartz diorites of the Marselevat granitoid seem to be the first solidification products, which developed either by fractional crystallization (FC) or assimilation-fractional crystallization (AFC) insofar as they are typically encountered in or very close to the boundary between the Marselevat granitoid and basic to intermediate volcanic rocks of the Çağlayan formation which it intrudes. Dioritic rocks of the Marselevat granitoid plot in the medium-K field, whereas the other samples from the Marselevat granitoid and all samples of the Sırtyayla granitoid plot in the high-K field in the K_2O versus silica diagram of Le Maitre et al. (1989), given in Fig. 5. On the other hand, samples of the Çamlıkaya granitoid plot mostly in the medium-K field and may represent an early stage of arc magmatism (Wilson, 1989). All subunits of the arc-related intrusive associations show evidence for pre-plate collision; i.e. arc setting in the R1–R2 diagram (Fig. 6) of Batchelor and Bowden (1985).

Some HFSE versus HFSE variation plots, for example, Zr vs. Nb, Y and Th, clearly indicate a good separation between the Çamlıkaya granitoid and the Sırtyayla-Marselevat granitoids in terms of arc maturation (Fig. 7). For example, rock samples from the Çamlıkaya granitoid always show decreasing Nb, Y and Th contents, regarded as the crustal contribution in magma genesis (Mason and Moore, 1982; Wilson, 1989; Rollinson, 1993). A similar case is also detected in HFSE/HFSE vs. LILE/LILE plots, such as Rb/Sr vs. Nb/Y and Ba/Rb vs. Zr/Nb (Fig. 7), in which the Çamlıkaya granitoid and the dioritic rocks of the Marselevat granitoid are always distinguished from others. The particularly high Zr/Nb ratio of the dioritic rocks of the Marselevat ganitoid may reflect a relative dilution in Nb content due to assimilation of basic to intermediate volcanic rocks, namely the Çağlayan formation. A MORB-normalized (Pearce, 1983) incompatible-element spider diagram for the arc-related intrusive association shows lesser amounts of elements of crustal origin, such as Rb, K, Ba, Th and Y, coupled with high amounts of mantle indicator elements, such as P and Ti (Mason and Moore, 1982; Wilson, 1989) in the early Cretaceous Çamlıkaya granitoid relative to Late Cretaceous to Early Palaeocene Sırtyayla and Marselevat units. Such a distribution pattern for MORB-normalized spider diagrams is convenient for identifying the early stage of the Çamlıkaya granodiorite in arc plutonism; that is, pre-mature arc. The Sırtyayla and Marselevat granitoids show a similar characteristic, which may reflect a mature stage of arc plutonism, especially in their relatively high K, Rb, Ba, Th and Y contents and lower P and Ti contents (Fig. 8). However, dioritic rocks of the Marselevat unit—or that which is possibly contaminated by the assimilation of basic to intermediate volcanic rocks of the Çağlayan Formation, or which solidified first from the magma—resembles the Çamlıkaya granodiorite.

5.2. Syn-collisional asniyor leucogranite

Total alkali vs. silica, AFM and K_2O vs. silica diagrams indicate a high-K calc-alkaline character for the Asniyor

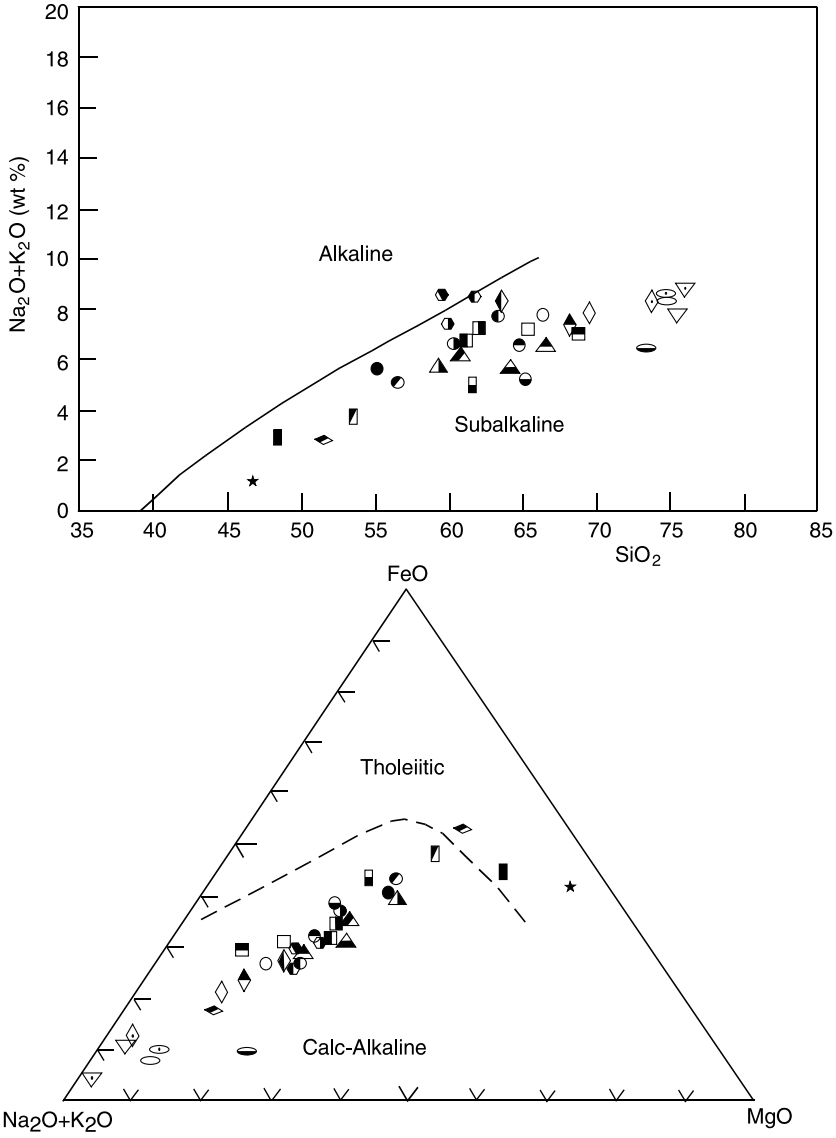

Fig. 4. Total alkali vs. silica and AFM diagrams (Irvine and Baragar, 1971) for rock samples from the Kaçkar batholith. See Fig. 3 for explanation.

leucogranite (Figs. 4 and 5) except for a few altered tonalites that plot in the low-K field due to K depletion. This leucogranite unit reflects a clear syn-collisional composition in the R1–R2 diagram (Fig. 6) of Batchelor and Bowden (1985). On the other hand, the geochemical behavior of tonalitic samples from the Asniyor leucogranite is always distinct from other rock types (Figs. 4–6).

Trace-element data for the syn-collisional Asniyor leucogranite show a characteristic behavior which distinguishes it from another leucocratic rock unit, the Sasmistal microgranite (Fig. 9). As mentioned above, the Sasmistal microgranite is considered to be a highly evolved derivative of the post-collisional, high-K, calc-alkaline Ayder K-feldspar megacrystic granitoid rather than a syn-collisional leucocratic igneous unit; additional evidence is provided below. Two subtrends are evident on the MORB-normalized spider diagram for the Asniyor leucogranite, belonging to the granitic-monzogranitic and tonalitic types of altered rocks, respectively (Fig. 10). The variation in Ba content of the granitic-monzogranitic subtrend is somewhat greater than that of the Sasmistal microgranite (see below). In the tonalitic subtrend, the effect of hydrothermal alteration is clearly evident in the considerably reduced K, Rb and Th, and elevated Sr contents (Fig. 10).

5.3. Post-collisional high-K calc-alkaline intrusive association

Major-element data show an apparent high-K calc-alkaline composition for the Ayder K-feldspar megacrystic granitoid and Sasmistal microgranite (Figs. 4 and 5). When plotted on the R1–R2 diagram of Batchelor and Bowden (1985), a transitional setting between post-collisional uplift and arc origin is evident (Fig. 6). As described by Pearce

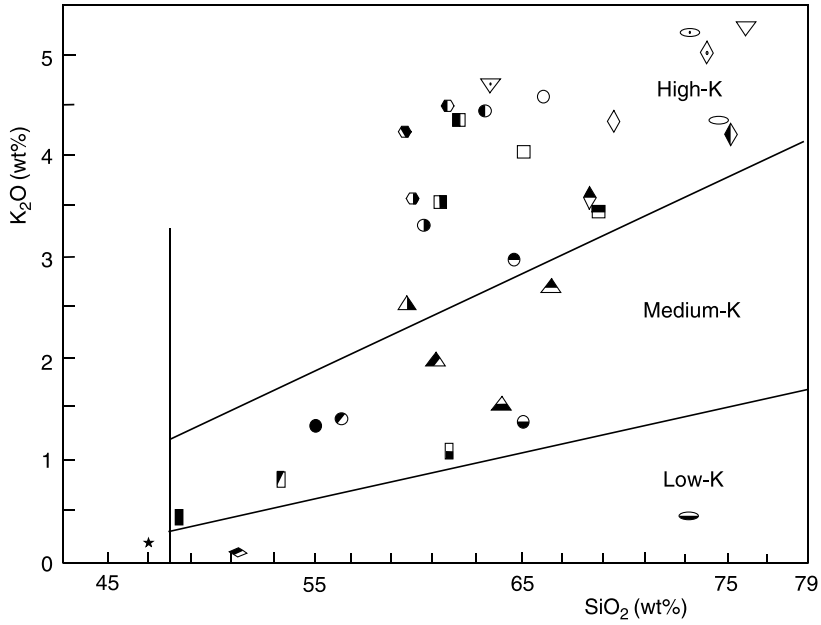

Fig. 5. K_2O vs. silica diagram (Le Maitre et al., 1989) for rock samples from the Kaçkar batholith. See Fig. 3 for explanation.

et al. (1984); Harris et al. (1986); Bonin (1990), arc- and post-collisional-related granitoids can overlap in these types of geochemical discrimination diagrams. This situation reflects mainly the inheritance characteristics of the source rocks melted in a post-collisional environment, which can be either old supracrustal or arc-related intracrustal rocks.

Trace-element data of the Ayder and Sasmistal units support the idea that the Sasmistal microgranite unit was derived from late-stage residual melts of the Ayder K-feldspar megacrystic granitoid. The Ayder and Sasmistal units seem to be the most enriched of all the units in the Kaçkar batholith in terms of LILE and HFSE contents (Fig. 9), except for Zr which is more enriched in the Güllübağ monzonite than in the other units (see below). MORB-normalized spider diagrams for the Ayder and Sasmistal units reveal a close relationship between these two rock units. However, the granitic rock of the Ayder unit shows some depletion in Sr, P and Ti (Fig. 10). In addition

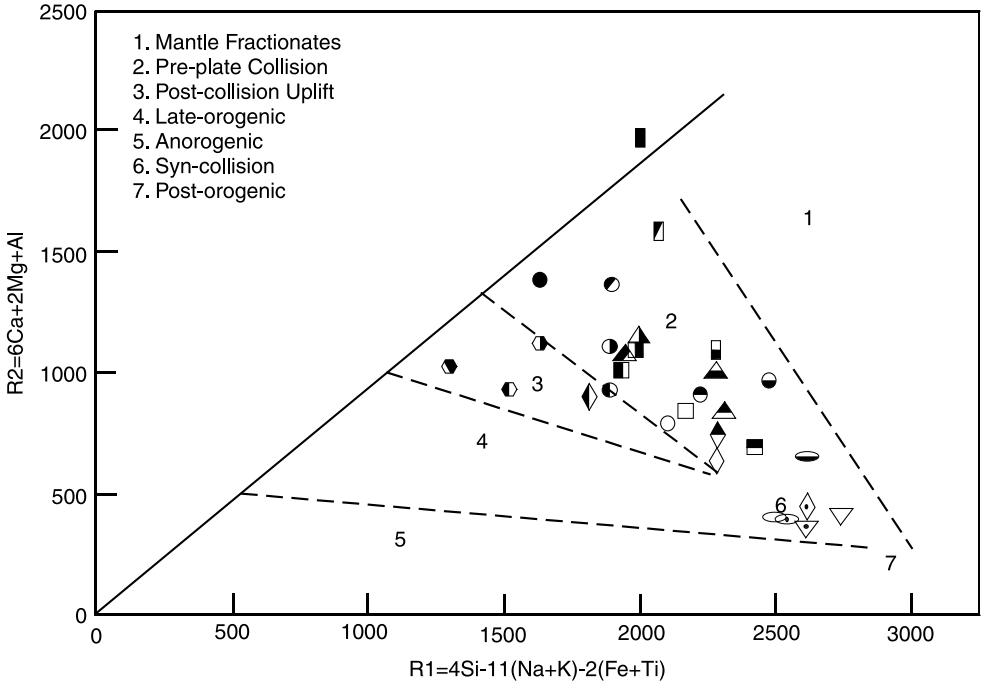

Fig. 6. R1–R2 major-element geotectonic discrimination diagram (Batchelor and Bowden, 1985) of rock samples from the Kaçkar batholith. See Fig. 3 for explanation.

to similar distribution patterns for MORB-normalized elements, slightly higher contents of some LILE such as K, Rb and Ba and lesser amounts of Sr in the Sasmistal microgranite relative to those of the Ayder K-feldspar megacrystic granitoid (Fig. 10) suggest late-stage derivation from a residual magma on the basis of petrogenetic considerations (Wilson, 1989; Rollinson, 1993). On the other hand, the high Th and Zr contents of the Sasmistal microgranite, as shown in a MORB-normalized spider diagram (Fig. 9), distinguish this unit from the other leucocratic granites, that is, the Asniyor leocogranite -a syn-collisional granitic intrusion.

5.4. Extension-related intrusive association

A total alkali vs. silica diagram indicates alkaline, transitional and subalkaline compositions for the monzonites, quartz monzonites and quartz monzodiorites, respectively, of the Güllübağ monzonite unit (Fig. 4). This unit possesses an apparent high-K character in the K_2O vs. silica diagram (Fig. 5) (Le Maitre et al., 1989). Data plotted on the R1–R2 geotectonic discrimination diagram (Fig. 6) clearly indicate a post-collisional setting for this unit. The Halkalıtaş quartz diorite follows a subalkaline to slightly tholeiitic trend as seen in Fig. 4, wherein diorite samples indicate early solidification within the tholeiitic field of Fig. 5. A mantle-dominant origin is also suggested by the K_2O content, which falls in the medium-K range in Fig. 6. Trace-element data in Fig. 9 reveal a distinct trend for the Güllübağ monzonite. However, this trend seems to be the continuation of another extensional-related intrusion, the Halkalıtaş quartz diorite. Apart from the association of trends for the Güllübağ and Halkalıtaş units in Fig. 9, the quantitative contents of various elements differ from one other; i.e. the Zr, Y and Th contents of the Güllübağ monzonite are higher than those of Halkalıtaş quartz diorite (Fig. 9). The Güllübağ monzonite seems to be enriched in all the LILE and HFSE (Fig. 11) relative to the Halkalıtaş quartz diorite. In particular, the low amounts of K, Rb, and Ba, and a monotonic decreasing trend from Ba to Y without any negative and positive anomalies in the MORB-normalized spider diagram for the Halkalıtaş quartz diorite, may be regarded as good evidence for a mantle-derived tholeiitic magma with a high degree of melting, or an early solidification product of the parent magma (Wilson, 1989; Rollinson, 1993) relative to those of the Güllübağ monzonite (Fig. 11).

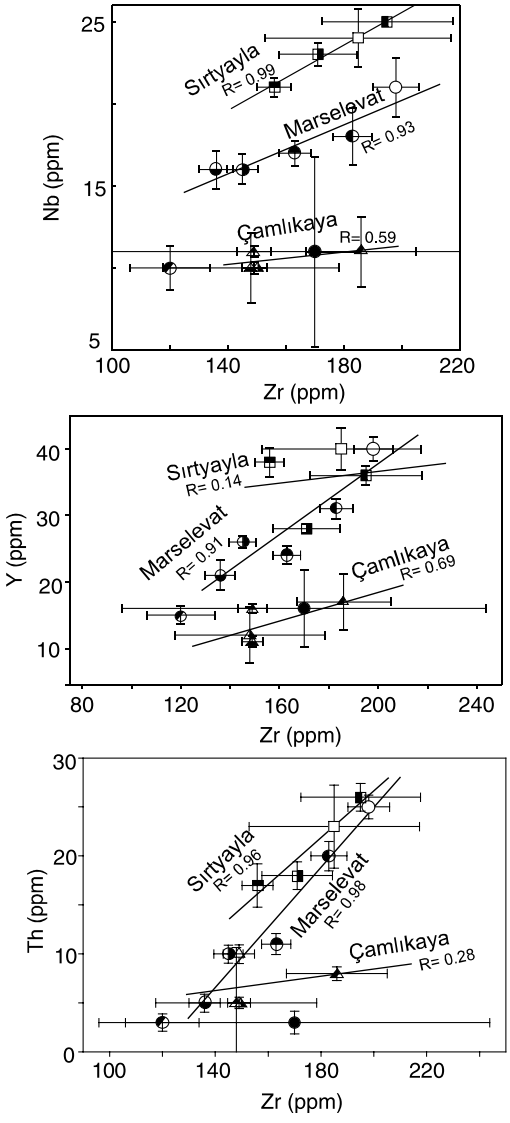

Fig. 7. Some LILE and HFSE variation diagrams for arc-related units from the Kaçkar batholith. See Fig. 3 for explanation.

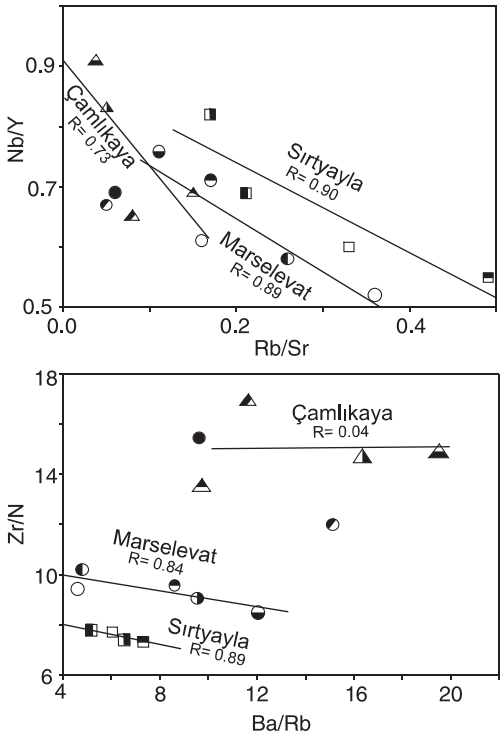

Fig. 7 (*continued*)

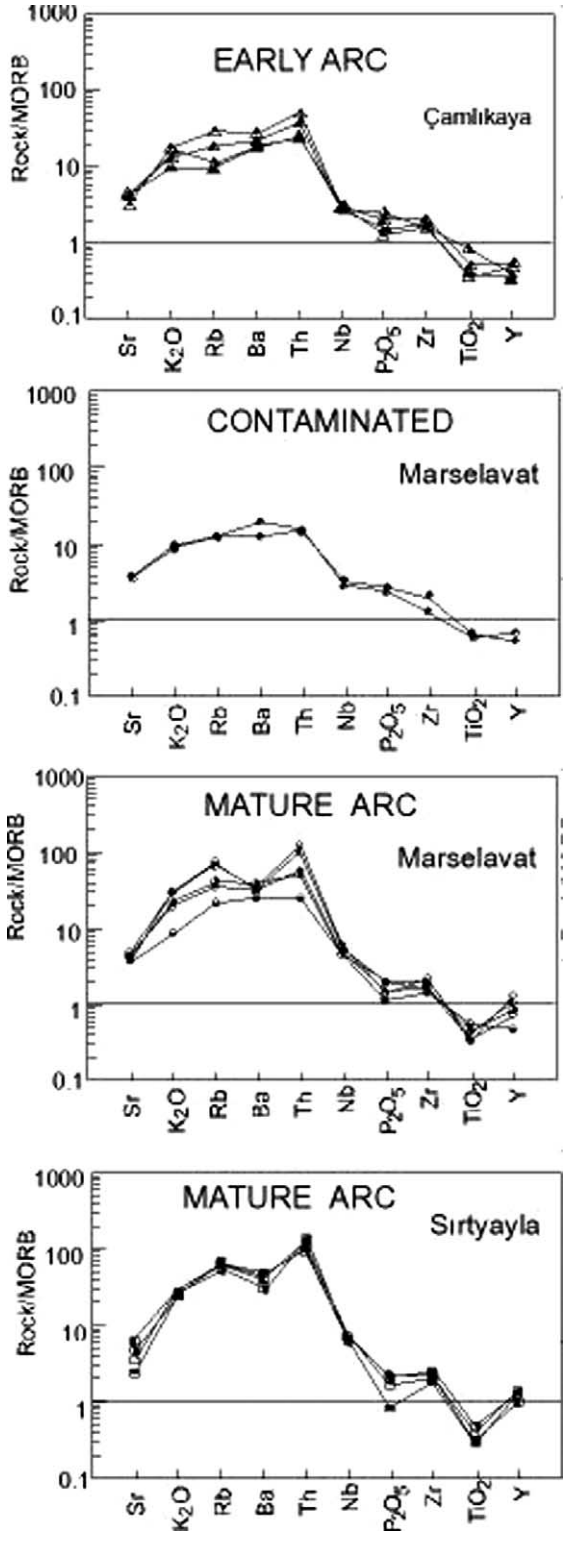

Fig. 8. MORB (Pearce, 1983) normalized spider diagram for rock samples from the arc-related units of the Kaçkar batholith. See Fig. 3 for explanation.

The Ardeşen gabbro and İsina diabase reveal an apparent low-K tholeiitic composition in Figs. 4 and 5. Trace-element data for the Ardeşen gabbro and İsina diabase differ from those of the other intrusive units in the Kaçkar batholith in terms of either less absolute abundances or distinct trends that reflect the mantle source (Fig. 9). Such a mantle-derived pattern is also seen in Fig. 11, which is similar to that of the Halkalıtaş quartz diorite, but differs from it in having slightly negative and positive anomalies in Ba and Zr, and Th and Ti contents, respectively.

6. Geodynamics

The Early Cretaceous Çamlıkaya granitoid and Late Cretaceous to Palaeocene Sırtyayla and Marselevat granitoids represent early and mature stages of arc plutonism, respectively. Different types of mafic microgranular enclaves and some special textures indicate magma mingling and magma mixing, reflecting voluminous

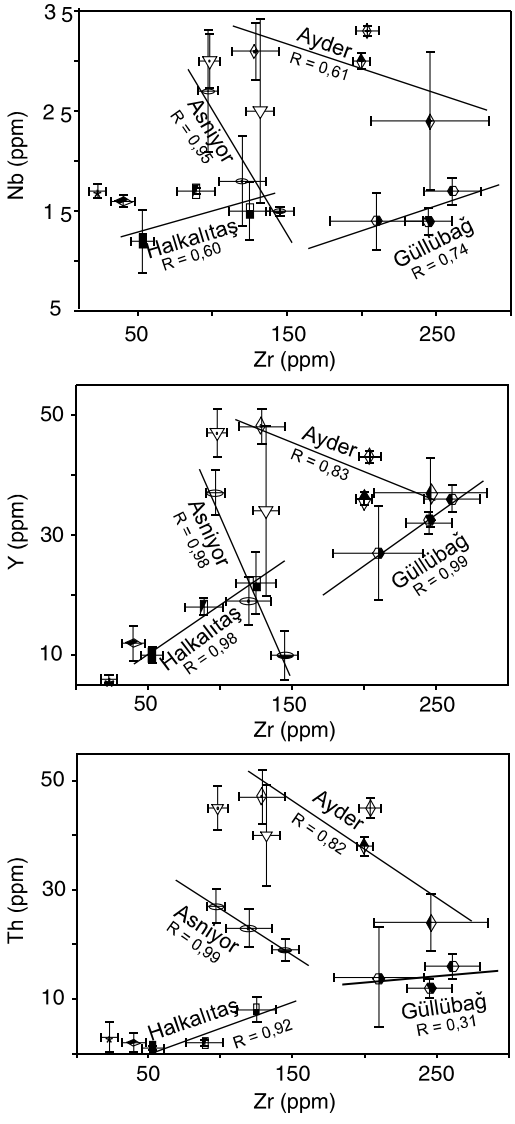

Fig. 9. Some LILE and HFSE variation diagrams for syn- to post-collisional- and extensional related units from the Kaçkar batholith. See Fig. 3 for explanation.

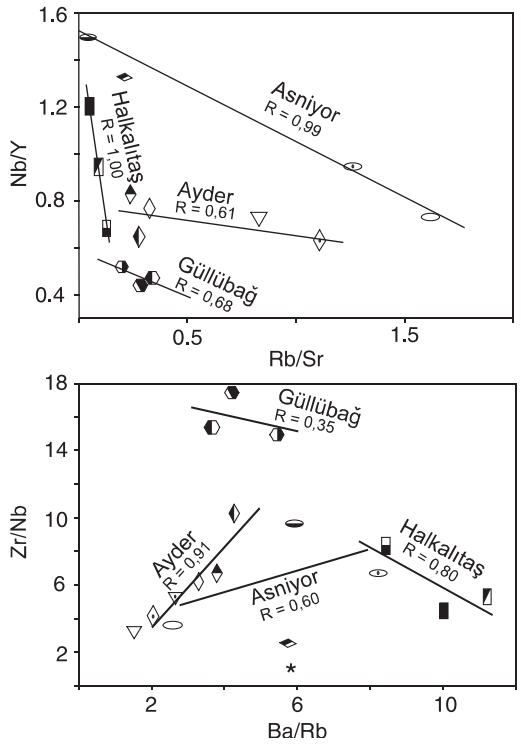

Fig. 9 (*continued*)

hybridization in the source region of the arc-related granodiorite units. A huge leucogranitic unit (Asniyor leucogranite), intruding both the Çamlıkaya and Marselevat granitoids, is suggested to be part of the syn-collisional magmatism resulting from collision of the EP and TAP in the Late Palaeocene–Early Eocene (Şengör and Yılmaz, 1981; Yılmaz et al., 1997; Okay and Şahintürk, 1997; Boztuğ et al., 2004). The Ayder granitoid and its highly-fractionated derivative, the Sasmistal microgranite, are the results of post-collisional high-K calc-alkaline magmatism. After crustal thickening due to Late Palaeocene-Early Eocene collision of the EP and TAP, there was a Middle Eocene regional extensional regime which developed in the eastern Black Sea region and accelerated the opening of the eastern Black Sea basin (Okay and Şahintürk, 1997; Kazmin et al., 2000). Thus, some small stocks and dikes constituting shallow-seated subvolcanic intrusions of Late Eocene age, such as the Güllübağ monzonite, Halkalıtaş quartz diorite, Ardeşen gabbro and İsina diabase units, are interpreted as products of a post-collisional, extension-related geodynamic setting. In fact, intrusion of these small and shallow-seated subvolcanic units with distinctive N–S, NE–SW, NW–SE and E–W orientations may also represent paleo-transcurrent fault zones in the crust where they were emplaced. According to Yılmaz et al. (1997), the Pontide mountain belt began to be uplifted as a giant horst block during the Late Miocene. Recent apatite fission-track data have also revealed tectonically rapid exhumation sometime around 20 Ma (work in progress).

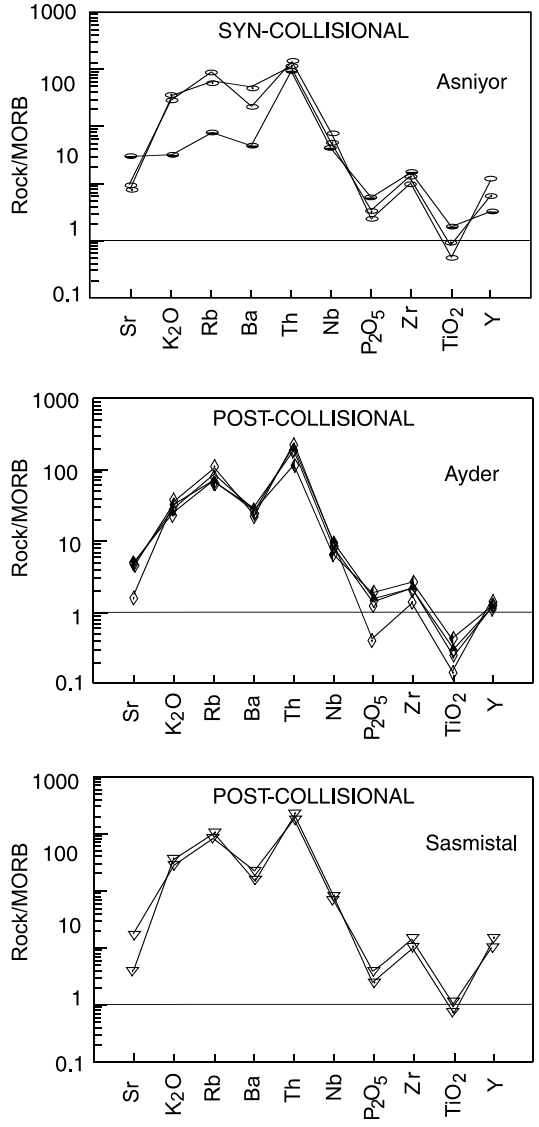

Fig. 10. MORB (Pearce, 1983) normalized spider diagram for syn- to post-collisional related units of the Kaçkar batholith. See Fig. 3 for explanation.

7. Discussion

The Late to Middle Eocene Ayder K-feldspar megacrystic granitoid typically bears large K-feldspar megacrysts as well as various kinds of mafic micro-granular, composite and even porphyritic enclaves with K-feldspar megacrysts, similar to those of their host rocks. These occurrences are considered to represent magma mingling and mixing that occurred at different depths during ascent of coeval felsic and mafic magmas. This granitoid unit may have been related to post-collisional lithospheric delamination that immediately followed the collision between EP and TAP in the eastern Pontides. As is well-known, lithospheric delamination can produce coeval felsic and mafic magmas derived either from crustal or mantle rocks whose mingling and mixing yield high-K hybrid rocks (Kay and Kay, 1993; Parada et al.,

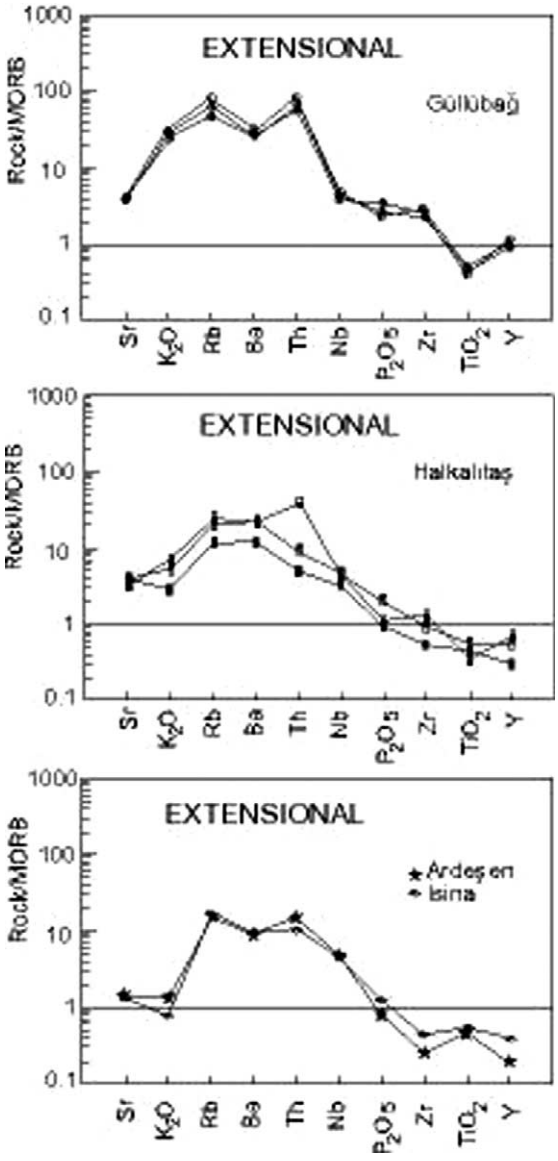

Fig. 11. MORB (Pearce, 1983) normalized spider diagram for extensional related units of the Kaçkar batholith. See Fig. 3 for explanation.

1999; Chen et al., 2000; Schofield and D'Lemos, 2000; Farmer et al., 2002; Acef et al., 2003). Such a post-collisional lithospheric delamination-related origin has already been proposed for the K-feldspar megacrystic I-type granitoids of central Anatolia, Turkey by Boztuğ, (1998, 2000), Düzgören-Aydın et al. (2001), and İlbeyli et al. (2004). Some EPMA mineral chemistry, as well as whole-rock Pb, Sr and Nd isotope geochemical data, are required to further assess contamination of the Marselevat granitoid magma by assimilation of basic volcanic rocks of the Çağlayan formation.

The dioritic and quartz dioritic rocks of the Marselevat granitoid are always exposed in the vicinity of basic volcanic rocks of the Çağlayan Formation. Such a geological setting suggests AFC processes in the genesis of the dioritic rocks of the Marselevat granitoid. The composition of the pluton may have been mainly governed by assimilation of basic volcanic rocks by magma, transforming it into dioritic composition during solidification, especially proximal to the boundary of the Marselevat granitoid and basic volcanic rocks of the Çağlayan Formation. Alternatively, these dioritic rocks may be the first FC derivatives of the Marselevat granitoid magma without any assimilation. Some EPMA mineral chemistry and isotope-geochemical data, such as Sr and Nd initial ratios, would be helpful in determining whether FC or AFC processes, or both, have occurred during solidification of the Marselevat granitoid. Some radioisotopic dating studies - such as U/Pb, Rb–Sr, K–Ar or Ar–Ar - as well as isotope-geochemical data are also needed in order to understand the igneous petrogenesis and geochronology of this large composite batholith in the eastern Pontides.

8. Conclusions

The composite Kaçkar batholith consists of five different magmatic associations, ranging from Early Cretaceous to Late Eocene in age, and from early to mature arc through syn- and post-collisional lithospheric delamination to post-collisional extension geodynamic settings. The oldest intrusive unit, Early Cretaceous in age, is unconformably overlain by the Turonian Ardıçlı Formation. The youngest intrusive units, Late Eocene in age, cut pre-Late Eocene intrusive units and are unconformably overlain by the Miocene Şebinkarahisar Formation. Some major NE-SW trending faults caused tectonic uplift of this huge composite batholith in the Miocene.

The main petrochemical characteristics reflect the early and mature stages of arc plutonism of Early and Late Cretaceous age, respectively. A huge leucogranite outcrop, mapped as the Asniyor leucogranite, intrudes the arc plutonic rocks and represents syn-collisional magmatism derived from the Late Palaeocene-Early Eocene collision of the EP and TAP. The Asniyor leucogranite is considered to be Palaeocene in age based on partial annealing of titanite fission-track ages of the Çamlıkaya granitoid caused by intrusion of the Asniyor leucogranite (Boztuğ et al., 2002). The Ayder K-feldspar megacrystic granitoid is considered to have been derived from post-collisional lithospheric delamination-related geodynamics immediately following collision of the EP and TAP in the eastern Pontides. Evidence for this interpretation include its Late to Middle Eocene age, mineralogical-petrographical characteristics and high-K CALK geochemical composition. After amalgamation of the EP and TAP, the post-collisional, extensional and intrusive association was accompanied by emplacement of small subvolcanic stocks and dikes during Late Eocene time. This association consists of four mappable lithological units having from mildly alkaline through medium-K tholeiite to low-K tholeiite

compositions. All of these intrusive associations represent various stages of a convergence system, i.e. subduction, syn-collision, post-collision and extension. These stages are related to northward subduction of the Neo-Tethyan ocean beneath the Eurasian plate along the Izmir-Ankara-Erzincan/Sevan-Akera suture zone and subsequently developing compressional and extensional tectonic regimes.

Acknowledgements

The authors thank Prof. Dr B. Sadıklar and Prof. Dr Mehmet Arslan (KTU, Trabzon, Turkey) for their constructive criticism of the original manuscript. Dr Greg B. Arehart (Univ. of Nevada, Reno) is kindly thanked for his correction of the English, and Dr Jennifer Lytwyn (Univ. of Houston, Dept. of Geosciences) has also helped us significantly through her improvement of our English expression. The Department of Geological Engineering, Cumhuriyet University (Sivas) has made possible the geochemical analysis of 401 rock samples.

References

Acef, K., Liegois, J.P., Ouabadi, A., Latouche, L., 2003. The anfeg post-collisional pan-african high-K calc-alkaline batholith (Central Hoggar, Algeria), result of the latea microcontinent metacratonization. Journal of African Earth Sciences 37 (3-4), 295–311.

Barbarin, B., Didier, J., 1992. Genesis and evolution of mafic microgranular enclaves through various types of interaction between coexisting felsic and mafic magmas. Royal Society of Edinburgh Transactions: Earth Sciences 83, 145–153.

Batchelor, B., Bowden, P., 1985. Petrogenetic interpretation of granitoid rock series using multicationic parameters. Chemical Geology 48, 43–55.

Bonin, B., 1990. From orogenic to anorogenic settings: evolution of granitoid suites after a major orogenesis. Geological Journal 25, 261–270.

Boztuğ, D., 1998. Post-collisional central anatolian alkaline plutonism Turkey. Turkish Journal of Earth Sciences 7, 145–165.

Boztuğ, D., 2000. S-I-A- types intrusive associations: geodynamic significance of synchronism between metamorphism and magmatism in Central Anatolia Turkey. The Geological Society London Special Publication, vol. 173, pp. 441–458.

Boztuğ, D., 2001. Suşehri (Sivas)—Gölköy (Ordu) arasında KAFZ'nun kuzey ve güney kesimlerindeki granitoyidlerin ve çevre kayaçlarının petrolojik incelenmesi. TÜBİTAK Projesi Raporu, 195Y001, Proje No: YDABÇAG-9, 113 s (yayınlanmamış), Sivas (in Turkish with English Abstract).

Boztuğ, D., Erçin, A.İ., Göç, D., Er, M., İskenderoğlu, A., Kuruçelik, M.K., Kömür, İ., 2001. Petrogenesis of the composite Kaçkar batholith along a north-south geotraverse between Ardeşen (Rize) and İspir (Erzurum) towns, eastern Black Sea region, Turkey. Fourth International Turkish Geology Symposium, (ITGS IV), 24–28 September 2001, Adana/Turkey, Abstracts, p. 210.

Boztuğ, D., Wagner, G.A., Erçin, A.İ., Göç, D., Yeğingil, Z., İskenderoğlu, A., Kuruçelik, M.K., Kömür, İ., Güngör, Y., 2002. Sphene and zircon fission-track geochronology unravelling subduction- and collision-related magma surges in the composite Kaçkar Batholith, eastern Black Sea region, Turkey. 1st International Symposium of the Faculty of Mines (İTÜ) on Earth Sciences and Engineering, 16–18 May 2002, Istanbul, Turkey, Abstracts, p.121.

Boztuğ, D., Kuşçu, İ., Erçin, A.İ., Avcı, N., Şahin, S.Y., 2003. Mineral deposits associated with the pre-, syn- and post-collisional granitoids of the neo-Tethyan convergence system between the Eurasian and Anatolian plates in NE and Central Turkey. In: Eliopoulos, D. (Ed.), Mineral Exploration and Sustainable Development. Millpress, Rotterdam, pp. 1141–1144.

Boztuğ, D., Jonckheere, R., Wagner, G.A., Yeğingil, Z., 2004. Slow Senonian and fast palaeocene-early eocene uplift of granitoids in the central eastern Pontides Turkey: apatite fission-track results. Tectonophysics 382 (3-4), 213–228.

Çamur, M.Z., Güven, İ.H., Er, M., 1994. Geochemistry of Eastem Pontide volcanics, Turkey: an example of multiple volcanic cycles in arc evolution. Intemational Volcanological Congress, IAVCEI, Ankara-1994, Abstracts, Theme 2: Subduction-Related Magmas.

Chen, C.H., Lin, W., Lu, H.Y., Lee, C.Y., Tien, J.L., Lai, Y.H., 2000. Cretaceous fractionated I-type granitoids and metaluminous A-type granites in SE China: the Late Yanshanian post-orogenic magmatism. Transactions of the Royal Society of Edinburgh: Earth Sciences 91, 195–205.

Debon, F., Le Fort, P., 1983. A chemical-mineralogical classification of common plutonic rocks and associations. Transactions of the Royal Society of Edinburgh: Earth Sciences 73, 135–149.

Didier, J., Barbarin, B., 1991. The different types of enclaves in granites-nomenclature. In: Didier, J., Barbarin, B. (Eds.), Enclaves and Granite Petrology. Developments in Petrology. Elsevier, Amsterdam, pp. 19–23.

Düzgören-Aydın, N., Malpas, W., Göncüoğlu, M.C., Erler, A., 2001. Post collisional magmatism in Central Anatolia Turkey: field, petrographic and geochemical constraints. International Geology Review 43 (8), 695–710.

Eğin, D., Hirst, D.M., 1979. Tectonic and magmatic evolution of volcanic rocks from the northern Harşit river area, NE Turkey. Proceedings of Geocome 1 (the 1st Geological Congress on the Middle East). Mineral Research and Exploration of Turkey (MTA) Publications, pp. 56–93.

Farmer, G.L., Glazner, A.F., Manley, C.R., 2002. Did lithospheric delamination trigger late cenozoic potassic volcanism in the southern Sierra Nevada, California. Geological Society of America Bulletin 114 (6), 754–768.

Gedik, A., Ercan, T., Korkmaz, S., Karataş, S., 1992. Rize-Fındıklı-Çamlıhemşin arasında (Doğu Karadeniz) yer alan magmatik kayaçların petrolojisi ve Doğu Pontidlerdeki bölgesel yayılımları. Türkiye Jeoloji Bülteni 35, 15–38 (in Turkish with English abstract).

Govindaraju, K., 1989. Compilation of working values and sample description for 272 geostandards. Geostandards Newsletter 13, 1–113.

Harris, N.B.W., Pearce, J.A., Tindle, A.G., 1986. Geochemical characteristcs of collision-zone magmatism. In: Coward, M.P., Ries, A.C. (Eds.), Collision Tectonics The Geological Society London, Special Publication, vol. 19, pp. 67–81.

Hibbard, M.J., 1991. Textural anatomy of twelve magma-mixed granitoid systems. In: Didier, J., Barbarin, B. (Eds.), Enclaves and Granite Petrology. Developments in Petrology 13. Elsevier, Amsterdam, pp. 431–444.

Hibbard, M.J., 1995. Petrography to Petrogenesis. Prentice-Hall, Englewood Cliffs, NJ.

Ilbeyli, N., Pearce, J.A., Thirwall, M.F., Mitchell, J.G., 2004. Petrogenesis of collision-related plutonics in central Anatolia Turkey. Lithos 72, 163–182.

Irvine, T.N., Baragar, W.R.A., 1971. A guide to the chemical classification of common volcanic rocks. Canadian Journal of Earth Sciences 8, 523–548.

Kay, R.W., Kay, S.M., 1993. Delamination and delamination magmatism. Tectonophysics 219 (1-3), 177–189.

Kazmin, V.G., Schreider, A.A., Bulychev, A.A., 2000. Early stages of evolution of the Black Sea. The Geological Society London, Special Publication 173, 235–249.

Korkmaz, S., Tüysüz, N., Er, M., Musaoğlu, A., Keskin, İ., 1995. Stratigraphy of the Eastern Pontides, NE Turkey. In: Erler, A., Ercan, T., Bingöl, E., Örçen, S. (Eds.), Geology of the Black Sea Region. Proceedings of the International Symposium on the Geology of the Black Sea Region, September 7–11, 1992, Ankara, Published by the General Directorate of Mineral Research and Exploration and Chamber of Geological Engineers, Ankara, Turkey, pp. 59–68.

Le Maitre, R.W., Bateman, P., Dudek, A., Keller, J., Lameyre, J., Le Bas, M.J., Sabine, A., Schmid, R., Sorensen, H., Streckeisen, A., Woolley, A.R., Zanettin, B., 1989. A classification of igneous rocks and glossary of terms; recommendations of the International Union of Geological Sciences Subcommission on the Systematics of Igneous Rocks, Blackwell.

Manetti, P.Y., Peccerillo, A., Poli, C., Corsini, F., 1983. Petrochemical constraints on models of cretaceous-eocene tectonic evolution of the eastern pontide chain (Turkey). Cretaceous Research 4, 159–172.

Mason, B., Moore, C.B., 1982. Principles of geochemistry. Wiley, Hong Kong.

Okay, A.I., Şahintürk, Ö., 1997. Geology of the Eastern Pontides. In: Robinson, A.G. (Ed.), Regional and Petroleum Geology of the Black Sea and Surrounding Region. AAPG Memoir, 68, pp. 291–311.

Parada, M.A., Nystrom, J.O., Levi, B., 1999. Multiple sources for the Coastal batholith of central Chile (31–34 degrees S): geochemical and Sr–Nd isotopic evidence and tectonic implications. Lithos 46 (3), 505–521.

Pearce, J.A., 1983. Role of the sub-continental lithosphere in magma genesis at active continental margins. In: Hawkesworth, C.J., Norry, M.J. (Eds.), Continental Basalts and Mantle Xenoliths. Shiva, Nantwich, pp. 230–249.

Pearce, J.A., Harris, B.W., Tindle, A.G., 1984. Trace element discrimination diagrams for the tectonic interpretation of granitic rocks. Journal of Petrology 25, 956–983.

Rollinson, H.R., 1993. Using Geochemical Data: Evaluation, Presentation, Interpretation, Longman Scientific and Technical. Wiley, New York.

Schofield, D.I., D'Lemos, R.S., 2000. Granite petrogenesis in the Gander Zone NE Newfoundland: mixing of melts from multiple sources and the role of lithospheric delamination. Canadian Journal of Earth Sciences 37 (4), 535–547.

Şengör, A.M.C., Yılmaz, Y., 1981. Tethyan evolution of Turkey: a plate tectonic approach. Tectonophysics 75, 181–241.

Streckeisen, A., 1976. To each plutonic rock its proper name. Earth Science Reviews 12, 1–33.

Tokel, S., 1992. Magmatic and geochemical evolution of the Pontide segment of the northern Tethys subduction system. In: Erler, A., Ercan, T., Bingöl, E., Örçen, S. (Eds.), Geology of the Black Sea Region. Proceedings of the International Symposium on the Geology of the Black Sea Region, September 7–11, 1992, Ankara. General Directorate of Mineral Research and Exploration and Chamber of Geological Engineers, Ankara, Turkey, pp. 163–170.

Wilson, M., 1989. Igneous Petrogenesis. Unwin Hyman, London.

Yeğingil, Z., Boztuğ, D., Er, M., Oddone, M., Bigazzi, G., 2002. Timing of neotectonic fracturing by fission-track dating of obsidian in-filling faults in the İkizdere-Rize area, NE Black Sea region Turkey. Terra Nova 14 (3), 169–174.

Yılmaz, S., Boztuğ, D., 1996. Space and time relations of three plutonic phases in the Eastern Pontides (Turkey). International Geology Review 38, 935–956.

Yılmaz, Y., Tüysüz, O., Yiğitbaş, E., Genç, Ş.C., Şengür, A.M.C., 1997. Geology of tectonic evolution of the Pontides. In: Robinson, A.G. (Ed.), Regional and Petroleum Geology of the Black Sea and Surrounding Region AAPG Memoir, vol. 68, pp. 183–226.

Yılmaz, A., Adamia, S., Chabukiani, A., Chkhotua, T., Erdoğan, K., Tuzcu, S., Karabıyıkoğlu, M., 2000. Structural correlation of the southern Transcaucasus (Georgia)—eastern Pontides (Turkey). The Geological Society London Special Publications 173, 171–182.